JCB Article

Wnt-5/*pipetail* functions in vertebrate axis formation as a negative regulator of Wnt/β-catenin activity

Trudi A. Westfall,[1] Ryan Brimeyer,[1] Jen Twedt,[1] Jean Gladon,[1] Andrea Olberding,[1] Makoto Furutani-Seiki,[2] and Diane C. Slusarski[1]

[1]Department of Biological Sciences, University of Iowa, Iowa City, IA 52242
[2]Kondoh Differentiation Signaling Project, Sakyo-ku, 606-8394 Kyoto, Japan

We provide genetic evidence defining a role for noncanonical Wnt function in vertebrate axis formation. In zebrafish, misexpression of Wnt-4, -5, and -11 stimulates calcium (Ca^{2+}) release, defining the Wnt/Ca^{2+} class. We describe genetic interaction between two Wnt/Ca^{2+} members, Wnt-5 (*pipetail*) and Wnt-11 (*silberblick*), and a reduction of Ca^{2+} release in Wnt-5/*pipetail*. Embryos genetically depleted of both maternal and zygotic Wnt-5 product exhibit cell movement defects as well as hyperdorsalization and axis-duplication phenotypes. The dorsalized phenotypes result from increased β-catenin accumulation and activation of downstream genes. The Wnt-5 loss-of-function defect is consistent with Ca^{2+} modulation having an antagonistic interaction with Wnt/β-catenin signaling.

Introduction

The Wnt family of growth factors and components of their signaling pathways have diverse roles in development and disease. Wnt signaling influences cell fate, migration, polarity, and neural patterning while inappropriate activation has been implicated in several human cancers (Huelsken and Birchmeier, 2001). The Wnt gene family can be grouped into mechanistically distinct classes based on overexpression assays. The canonical Wnt class (also referred to as Wnt/β-catenin) consists of the *Drosophila wingless* (*wg*) and vertebrate Wnt-1 and -8 (Dale, 1998). In zebrafish and *Xenopus* embryos, overexpression of canonical Wnts induce hyperdorsalization and ectopic axes (Moon et al., 1993b; Du et al., 1995; Kelly et al., 1995; Moon and Kimelman, 1998). Stimulation of the canonical Wnt path activates a cytoplasmic phosphoprotein (dishevelled [dsh]), which then inhibits the function of a degradation complex including glycogen synthase kinase 3 and Axin. Down-regulation of glycogen synthase kinase 3 activity leads to accumulation of β-catenin, a multifunctional protein that interacts with cadherins as well as transcription factors (lymphoid enhancer factor/T-cell factor, DNA binding proteins) influencing gene expression (Bienz and Clevers, 2003). In addition, canonical Wnt signaling may be regulated by events Gsk-independent but Axin-dependent to modulate β-catenin nuclear entry (Tolwinski et al., 2003). The end result is tight regulation of Wnt/β-catenin activity and downstream target genes.

The common element of noncanonical Wnt signaling is that this class (including *Wnt-5A*, *-4*, and *-11*) appears to be β-catenin–independent (Kuhl et al., 2000b). Noncanonical Wnt activity can be viewed as a complex network with several cellular outputs identified by calcium (Ca^{2+}) modulation and polarized cell movement (Wnt/Ca^{2+} and planar cell polarity [PCP]; Mlodzik, 2002). Stimulation of the Wnt–Ca^{2+} pathway triggers the release of Ca^{2+} (Slusarski et al., 1997a,b), activating Ca^{2+} sensitive proteins including PKC (Sheldahl et al., 1999), Ca^{2+}/calmodulin-dependent kinases (CaMKII; Kuhl et al., 2000a) and calcineurin-dependent nuclear factor of activated T cells (Saneyoshi et al., 2002). More recently, a PCP-specific component, Prickle, has been shown to modulate cell movement and stimulate Ca^{2+} release in zebrafish, and a PCP-specific form of dsh has been shown to activate the Wnt/Ca^{2+} cascade in *Xenopus* and zebrafish (Sheldahl et al., 2003; Veeman et al., 2003). This work raises the intriguing possibility that Wnt/Ca^{2+} and PCP either substantially overlap or are part of the same signaling network.

In zebrafish, overexpression of *Xwnt-5A* is antagonistic to the Wnt/β-catenin class in that coinjection of RNA encoding

Address correspondence to Diane C. Slusarski, Dept. of Biological Sciences, 312 Biology Building, University of Iowa, Iowa City, IA 52242. Tel.: (319) 335-3229. Fax: (319) 335-1069. email: diane-slusarski@uiowa.edu

Key words: dorsal–ventral patterning; calcium; zebrafish; morphogenesis; signal transduction

Abbreviations used in this paper: Ca^{2+}, calcium; CaMKII, Ca^{2+}/calmodulin-dependent kinase; dsh, dishevelled; D-V, dorsal-ventral; hpf, hours post fertilization; IP_3R, inositol 1,4,5-triphosphate receptor; mz, maternal-zygotic; *ppt*, *pipetail*; *slb*, *silberblick*; YSL, yolk syncytial layer; XeC, Xestospongin C.

The Journal of Cell Biology, Volume 162, Number 5, September 1, 2003 889–898
http://www.jcb.org/cgi/doi/10.1083/jcb.200303107

Wnt-8 with Wnt-5A inhibits the dorsalizing effects of Wnt-8 overexpression. Stimulating Ca^{2+} release with activated serotonin receptor also antagonized Wnt-8 induced expansion of the dorsal domain (Slusarski et al., 1997b), suggesting that Wnt-5 antagonism of Wnt/β-catenin is downstream of the receptor–ligand interaction and mediated by Ca^{2+} release. Consistent with an antagonistic role, expression of antisense Wnt-5A in mammalian cell lines mimics Wnt-1 mediated transformation (Olson and Gibo, 1998). Furthermore, *Drosophila* Wnt 4 (*Dwnt-4*) is antagonistic to *wg* as injection of antisense *Dwnt-4* RNA resembles *wg* gain-of-function mutations and *Dwnt-4* antagonizes *wg* in *Xenopus* axis-inducing assays (Gieseler et al., 1999; Buratovich et al., 2000). *Dwnt-4* also functions in cell movement (Cohen et al., 2002). Misexpression of zebrafish Wnt-5 and Wnt-4 alters morphogenetic movements (Ungar and Moon, 1995; Slusarski et al., 1997b) and genetic mutations in zebrafish Wnt-5/*pipetail (ppt)* and Wnt-11/*silberblick (slb)* have been shown to influence convergence extension movements during gastrulation (Heisenberg et al., 2000; Kilian et al., 2003). Thus, in both vertebrates and invertebrates, noncanonical Wnts have dual functions; they are antagonistic to canonical Wnt signaling and modulate cell movement/polarity.

Although there is genetic and biochemical evidence for how the Wnt–β-catenin pathway works in both vertebrates and invertebrates, there is little genetic evidence for how noncanonical Wnt signaling pathways work in axis formation in vertebrates. Our paper provides a genetic demonstration of a maternal requirement for a Wnt in vertebrate dorsal-ventral (D-V) patterning. We identify zebrafish Wnt/Ca^{2+} class members (Wnt-4, -5, and -11) by virtue of their ability to stimulate Ca^{2+} release and demonstrate genetic interaction between Wnt-5/*ppt* and Wnt-11/*slb*. We show that manipulation of Wnt-5 activity by either gain-of-function or loss-of function results in changes in endogenous Ca^{2+} activity, and we can obtain partial rescue of the Wnt-5/*ppt* mutant with overexpression of a proposed downstream Ca^{2+}-sensitive protein, Ca^{2+}/calmodulin-dependent kinase (CaMKII). Through loss-of-function analyses, our data demonstrate an increase in β-catenin accumulation and activation of downstream genes supporting a functional role for Wnt/Ca^{2+} antagonism of Wnt/β-catenin activity in vertebrate development.

Results

Identification of zebrafish Wnt/Ca^{2+} members

Zebrafish embryos overexpressing Wnt-5A produce developmental defects similar to those induced by agents that stimulate phosphatidylinositol cycle activity (Slusarski et al., 1997b). Stimulation of the phosphatidylinositol cycle leads to intracellular Ca^{2+} release. Using in vivo image analysis in zebrafish, we demonstrated that *Xenopus* Wnt-5A overexpression increases Ca^{2+} release frequency twofold over endogenous levels (Slusarski et al., 1997b). We now ask if the *zebrafish Wnt* genes modulate Ca^{2+} release. Zebrafish embryos microinjected with a Ca^{2+}-sensitive dye along with the respective RNA are subjected to image analysis. Overexpression of zebrafish noncanonical Wnts (Wnt-4, -5, and -11) is sufficient to increase the frequency of Ca^{2+} release at least twofold over endogenous levels (zWnt-11; Fig. 1 A). Conversely, the canonical Wnt-8 does not change the levels of Ca^{2+} release relative to endogenous levels (Fig. 1 B). The Wnt-8 RNA is translated into a functional product in this assay as it induced dorsalization. The differential ability of the Wnt classes to modulate Ca^{2+} release is consistent with our earlier studies with Wnts and Frizzleds from other species (Slusarski et al., 1997a,b; Ahumada et al., 2002). Given that subtle differences in the amplitude and/or frequency of Ca^{2+} release can have profound effects on cell behavior (Berridge et al., 1998), we next characterized the impact Wnt-5-stimulated Ca^{2+} release on embryonic patterning.

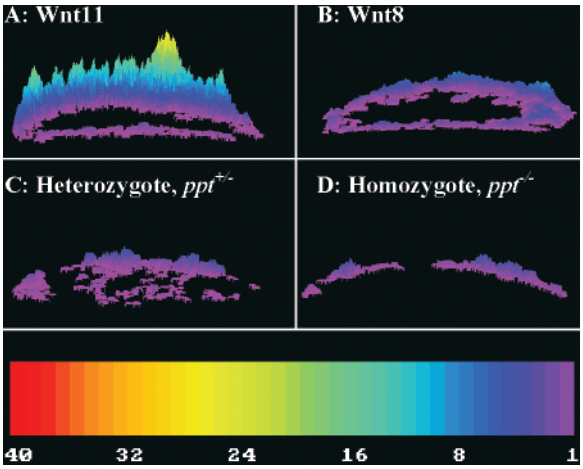

Figure 1. **Ca^{2+} release dynamics in zebrafish embryos expressing Wnts and in Wnt-5/*ppt* mutants.** Non-canonical Wnt members stimulate Ca^{2+} release in zebrafish and these changes were monitored with Fura-2 in live embryos. The representative embryo shown is a two-dimensional topographic image of the location of all the Ca^{2+} fluxes that occurred during the time course (50 min). Surface plots of Ca^{2+} release activity in embryos mis-expressing (A) Wnt-11 and (B) Wnt-8 RNA. Ca^{2+} release profile of endogenous activity in (C) heterozygous ($ppt^{+/-}$) and (D) mutant ($ppt^{-/-}$) embryos from the same clutch. Height and color of peaks indicate the number of Ca^{2+} fluxes observed over the course of the experiment with the embryos oriented in a lateral position. The color bar indicates the pseudocolor representation of the number of transients from low (purple, 1) to high (red, 40).

Ventralization phenotypes with Wnt-5 gain of function

For gain-of-function analyses, we manipulated Wnt-5 activity by DNA or RNA injections into wild-type embryos and subsequently monitored Ca^{2+} release frequency. In this manner, we can correlate the immediate physiological output of Ca^{2+} release with morphological or molecular changes evaluated hours later. Wnt-5 RNA injected embryos typically demonstrated robust early Ca^{2+} release activity (from 64- to 1,000-cell) resulting in cell movement defects as described in Slusarski et al. (1997b) and is consistent with morphogenetic defects described for zebrafish Wnt 4 (Ungar and Moon, 1995) and *Xenopus* Wnt-5A (Moon et al., 1993a). At the highest RNA concentrations, we induce hyperdorsalization defects (unpublished data) consistent with phenotypes described for high dose injections (>100 pg/embryo) in zebrafish (Kilian et al., 2003). Because we have

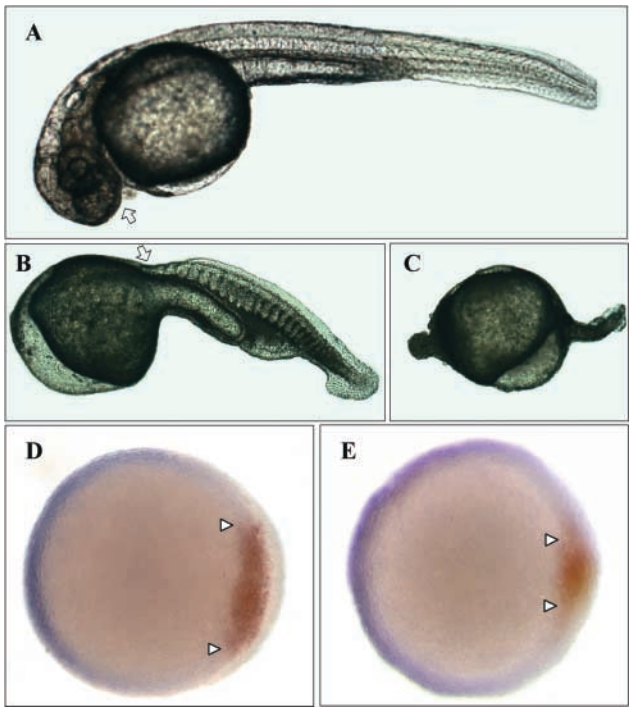

Figure 2. **Hyperventralization phenotypes of Wnt-5–injected embryos.** Embryos mis-expressing Wnt-5 were evaluated for changes in D-V patterning by morphology and whole mount in situ. (A) Wild-type morphology with the arrow designating the anterior-most region. Loss of dorsal-anterior tissue and expansion of ventral-posterior tissue is evident by lack of head tissue arrow in B and an onion-like mass of ventralized tissue in C. Dual-hybridization whole mount in situ at shield stage with the dorsal-specific chordin domain (red) denoted by arrowheads flanked by the ventral-specific eve (blue) expression domain. Reduction of dorsal domains and expansion of ventral domains compared with (D) wild-type is seen in (E) Wnt-5-injected embryos. (A–C) Lateral orientation with anterior to the left and (D–E) animal pole orientation with dorsal to the right.

demonstrated that depletion of intracellular Ca^{2+} stores in zebrafish embryos is sufficient to generate hyperdorsalized phenotypes (Westfall et al., 2003), we were concerned about Ca^{2+} depletion upon overexpression of Wnt-5 RNA. To this end, we used doses that stimulate a sustained, yet less robust, Ca^{2+} release frequency during development and in doing so with Wnt-5 DNA, we generated a range of phenotypes, including cell movement defects and ventralization as evaluated by morphology (Fig. 2, B and C) and by whole mount in situ (Fig. 2 E). Wnt-5 DNA injection into embryos is sufficient to activate Ca^{2+} release just before and beyond 1,000-cell stage. Hyperventralization is demonstrated by reduction of dorsal anterior tissue (Fig. 2 B) and expansion of ventral posterior tissue with the most severe phenotype resembling an onionlike morphology of ventralized tissue (Fig. 2 C). Molecular analysis at 60–80% epiboly demonstrates a reduction of the presumptive dorsal region (labeled by chordin; Miller-Bertoglio et al., 1997) and expansion of presumptive ventral tissue (marked by eve1; Fig. 2 E; Joly et al., 1993) when compared with control-injected embryos (Fig. 2 D). The potency of the Wnt5 ligand is evident as relatively minor dose changes (of both RNA and DNA) have a profound impact on the frequency of Ca^{2+} release with a concomitant range of developmental defects. Although Wnt-5 misexpression implicates a role in D-V patterning, we wanted to confirm with loss-of-function analyses.

Genetic interaction between zebrafish Wnt-5 (*ppt*) and Wnt-11 (*slb*)

Genetic mutations have been isolated for Wnt-5 and -11 (Rauch et al., 1997; Heisenberg et al., 2000). Given that both are expressed in the early embryo and capable of stimulating Ca^{2+} release, we decided to test for genetic interaction. The *slb* mutation maps to Wnt-11 and molecular analysis revealed that an extreme allele, slb^{tz216}, was a loss-of-function allele (Heisenberg et al., 2000). *ppt* maps to the *Wnt-5* gene and the most severe allele (ppt^{ti265}) phenotypically has a premature stop codon eliminating three conserved cysteines in the COOH terminus (Rauch et al., 1997). Due to the fact that the ppt^{ti265} mutation is a truncation, we wanted to verify that the ppt^{ti265} allele was not antimorphic. Expression of ppt^{ti265} mRNA in wild-type embryos did not generate any $ppt^{-/-}$ mutant phenotypes (unpublished data) leading us to conclude that ppt^{ti265} is a loss-of-function mutation.

The *slb* mutation affects forebrain patterning and homozygous slb^{tz216} mutant embryos often have incomplete separation of the eyes (Fig. 3 B, arrow pointing to a fused lens) compared with wild-type (Fig. 3 A). Homozygous ppt^{ti265} mutant embryos display shortened body length and undulating notochords but most commonly tail defects (deformed tip of tail resembling a pipe; Fig. 3 C, arrow). To test for genetic interaction, we generated adult fish doubly heterozygous for ppt^{ti265} and slb^{tz216} and crossed to obtain doubly homozygous mutant embryos, confirmed by PCR of genomic DNA. The double homozygous mutant embryo phenotype is markedly more severe than the additive of the single mutant combinations. The eye anlagen fuse more frequently in the double mutant embryos than in $slb^{-/-}$ embryos (Fig. 3 D). Double homozygous mutant embryos also have more severe tail and trunk defects than observed in $ppt^{-/-}$ (Fig. 3 D).

Reduced Ca^{2+} release in Wnt-5 (*ppt*) mutant embryos

Given that Wnt-5 misexpression is sufficient to modulate Ca^{2+} release and induce ventralization, we next ask if Wnt-5 function is necessary for endogenous Ca^{2+} release activity in embryos. In vivo image analysis of Ca^{2+} release identifies a reduced frequency in $ppt^{-/-}$ embryos (Fig. 1 D, average of 0.76 new transients/min) compared with $ppt^{+/-}$ siblings (Fig. 1 C, average of 1.2 new transients/min). Interestingly, the embryonic region displaying the greatest reduction of Ca^{2+} activity in $ppt^{-/-}$ embryos includes the yolk syncytial layer (YSL). The embryos are imaged in a lateral orientation and the YSL region would be included in the bottom portion of the half-moon–like topographical plot and note the lack of transients in that region (Fig. 1 D). The YSL has been shown to play important roles in epiboly, early induction and patterning in zebrafish (for review see Sakaguchi et al., 2002).

Alterations in cell movement have been described in *slb* mutant embryos (Heisenberg and Nusslein-Volhard, 1997; Heisenberg et al., 2000) and in embryos homozygous for an

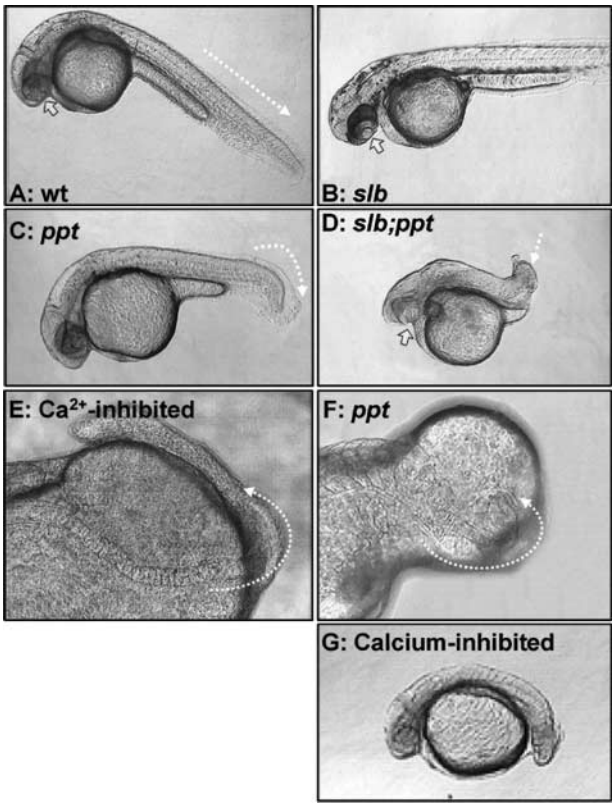

Figure 3. **Morphological phenotypes in Wnt-5/*ppt* and Ca^{2+}-inhibited embryos.** Lateral view, anterior to the right of 24–36 hpf embryos. (A) In wild-type, the block arrow indicates one eye, the other is out of the focal plane and the dashed lined demarcates the tail extending posteriorly off the yolk. (B) The Wnt-11 mutant ($slb^{-/-}$) embryo has a fused eye, the arrow indicates the lens. (C) In Wnt-5 mutant ($ppt^{-/-}$), the dashed arrow demarcates the shortened-curled tail defect and in the (D) double mutant ($slb^{-/-}$; $ppt^{-/-}$), the block arrow indicates the fused eye, whereas the dashed arrow marks the shortened-twisted tail. The notochord and one set of somites are highlighted by a dashed line in (E) IP_3R-inhibited (XeC), and (F) $ppt^{-/-}$ embryos. The presence of a protruding yolk is an indication of incomplete epiboly cell movements. Fused eyes and shortened twisted trunks can also be observed in (G) Ca^{2+}-inhibited (L-690,330-treated) embryos.

allele of *ppt* that replaces one conserved cysteine (ppt^{ta89}) leaving the rest of the Wnt-5 sequence intact (Heisenberg et al., 2000; Kilian et al., 2003). In addition to the prototypical *ppt* tail defect (Fig. 3 C), we also observe some epiboly defects in the ppt^{ti265} allele genetic background. As the ppt^{ti265} is the most severe allele identified thus far, we believe it uncovers additional roles for Wnt-5 in cell movement. Consistent with altered Ca^{2+} modulation in $ppt^{-/-}$ embryos contributing to the mutant phenotypes is the fact that we reproduce, in part, the phenotypic defects in Ca^{2+} release suppressed embryos. Late treatments with phosphoinositide cycle inhibitors (after 128–256 cell stage) result in anterior brain defects and eye fusions similar to those described for *slb* (Westfall et al., 2003). We target phosphoinositide cycle turnover with L-690,330 and block Ca^{2+}release from inositol 1,4,5-triphosphate receptor (IP_3R) channels with Xestospongin C (XeC; Atack et al., 1993; Gafni et al., 1997). Inhibitor-treated embryos were analyzed for in vivo Ca^{2+} release dynamics and we selected a dose that approximately mimics the reduced Ca^{2+} release frequency observed in $ppt^{-/-}$ embryos. In both Ca^{2+} release–inhibited (Fig. 3 E) and in $ppt^{-/-}$ (Fig. 3 F) embryos, we observe cell movement defects resulting in split somites encircling the yolk typically fusing back together at the most posterior tip of the tail. We also observe twisted posterior notochord defects, thus, contorting the tail similar to $ppt^{-/-}$ phenotypes and also generated embryos with trunk and tail defects similar to $ppt^{-/-}$;$slb^{-/-}$ phenotypes (Fig. 3 G).

Maternal depletion of Wnt-5 (*ppt*) reveals a necessary role in ventral patterning

Strong inhibition of IP_3R function with blocking antibodies leads to expanded dorsal structures in *Xenopus* (Kume et al., 1997). Consistent with the *Xenopus* studies, inhibition of either IP_3R or phosphoinositide cycle turnover results in hyperdorsalization in zebrafish (Westfall et al., 2003). In comparison, we use relatively mild doses of inhibitor (XeC and L-690,330) to match the reduced Ca^{2+} release frequency in the zygotic $ppt^{-/-}$ embryos. This raises the possibility that there may be residual Wnt-5 in these zygotic $ppt^{-/-}$ embryos. In support of this notion, Wnt-5 transcript is maternally deposited and ubiquitously expressed in zebrafish (Blader et al., 1996) but protein distribution is unknown. Antisense morpholino knockdown of Wnt-5 generates phenotypes similar to the zygotic mutant (Lele et al., 2001). It should be noted that the antisense approach does not eliminate maternal protein. Therefore, in order to determine if maternally supplied Wnt-5 is contributing to early patterning, we set out to generate $ppt^{-/-}$ females by gene product rescue.

Assuming that maternal product would be present in embryos from a heterozygous *ppt* cross, we injected Wnt-5 DNA (~200 pl of 10–12 ng/ul) at a concentration that activates mild yet sustained Ca^{2+} release. We score rescue by suppression of the *ppt* morphological phenotypes. Injection sets with less than 10% *ppt*-like phenotypes, compared with 25% phenotypes in clutch controls, were allowed to develop. A small number of the rescued embryos developed swim bladders, a necessary organ for zebrafish viability and were raised to adulthood. Mature $ppt^{-/-}$ females were PCR genotyped.

Consistent with maternal effect mutations, embryos collected from $ppt^{-/-}$ females exhibit phenotypes regardless of the paternal genotype. Embryos from $ppt^{-/-}$ females crossed to heterozygous $ppt^{+/-}$ males fell into two general phenotypic groups. One class, accounting for >50% of the defects, is similar to the tail defects observed in mutant embryos from heterozygous females (Fig. 4 B), however, embryos from $ppt^{-/-}$ females have pointedly more severe defects with extreme shortened axis, undulating notochord and tail defects (Fig. 4 C). This class of phenotypes was scored as *ppt*-zygotic–like. The other phenotypic group (38%, 193/506) demonstrated dorsalized mutant phenotypes similar to those described in Mullins et al. (1996), as well as axis duplication phenotypes. These include expansion of somites, shortened and twisted tail (*piggy-tail*–like; Fig. 4 D) and severe curling of the tail over the trunk (*snail-house*–like; Fig. 4 F) instead of straight extension off of the yolk as in wild-type (Fig. 4, A and E). The $ppt^{-/-}$ embryo in Fig. 4 G has a partial secondary axis with an ectopic pair of otic vesicles associated with a duplicated beating heart. Organ duplication was verified in several maternal-

zygotic *ppt*$^{-/-}$ (mz*ppt*) embryos by whole mount in situ with a cardiac specific probe (Fig. 4 I; Chen and Fishman, 1996). Based on morphology, the hyperdorsalized and duplicated axis defect frequency of 38% is consistent, yet lower than the expected 50% frequency for embryos depleted of both maternal and zygotic product. The lower frequency could be the result of a maternal effect that is not fully penetrant or that we were conservative in scoring a phenotype as dorsalized and instead classified it as a severe *ppt*-zygotic–like defect. To distinguish between these two possibilities, we employed a more sensitive molecular analysis of dorsal patterning.

Wnt-5 (*ppt*) maternal phenotypes are the result of ectopic dorsal signaling centers

The hyperdorsalization and partial secondary axis phenotypes observed in maternally depleted *ppt* embryos suggest an expanded and/or ectopic dorsal signaling center. Confirmation that loss of Wnt-5 function results in expansion of dorsal tissue was obtained by whole mount in situ hybridization analysis with the dorsal-specific probe *chordin* (Miller-Bertoglio et al., 1997). In wild-type embryos, chordin is typically expressed in the shield region at 6 h post fertilization (hpf; Fig. 4 J, white arrowheads). 64% of the embryos (n = 73) from *ppt*$^{-/-}$ females crossed to *ppt*$^{+/-}$ males display expanded (Fig. 4 K) and/or ectopic (Fig. 4 L) domains of *chordin* expression.

Maternal loss of Wnt-5 (*ppt*) results in β-catenin stabilization

One mechanism leading to the dorsalization phenotypes described in the previous paragraph is activation of the canonical Wnt path leading to accumulation of β-catenin protein. Although there is no evidence for a maternal canonical Wnt ligand in zebrafish, there is nuclear accumulation of β-catenin protein on the future dorsal side

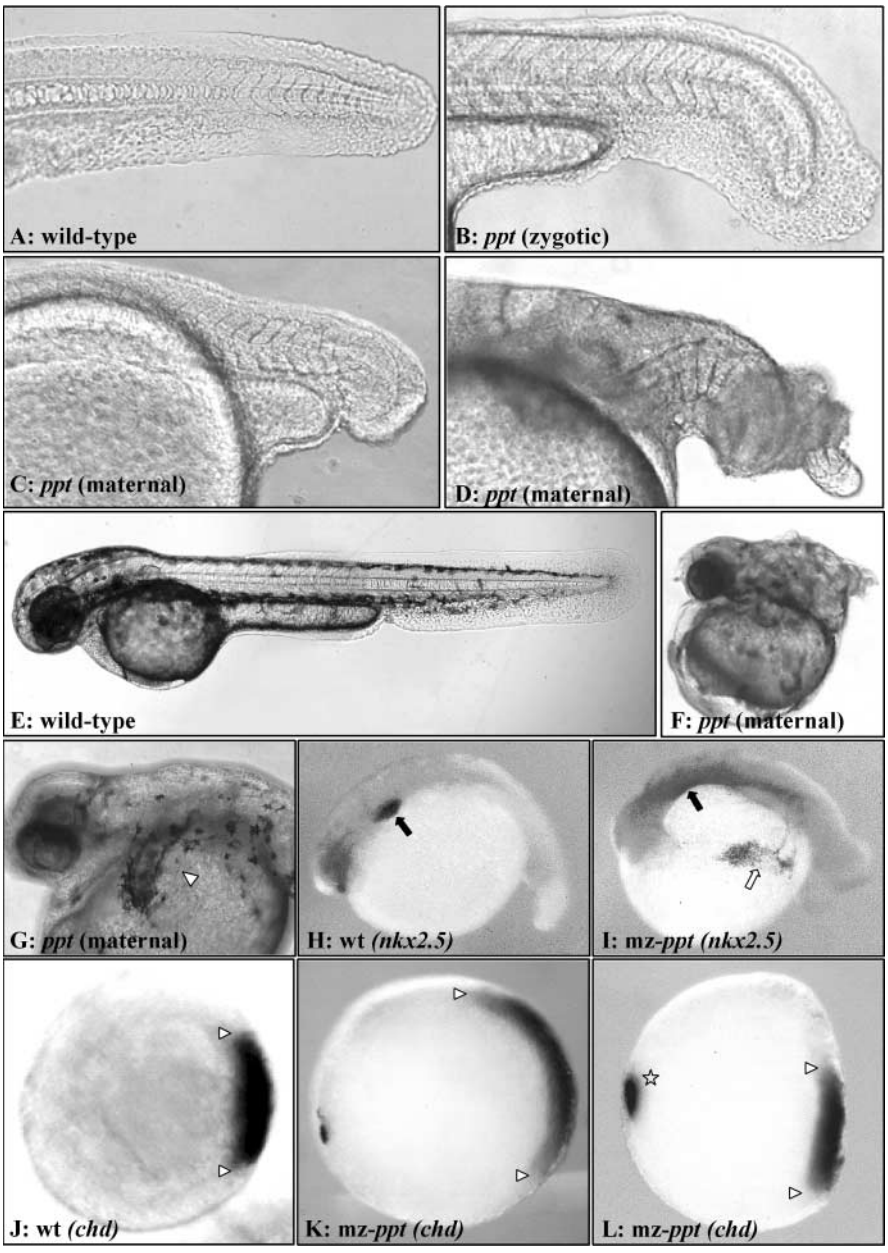

Figure 4. **Phenotypes of Wnt-5/*ppt* maternal-depleted embryos.** Tail and trunk morphology in (A and E) wild-type, (B) zygotic *ppt*$^{-/-}$, and embryos collected from *ppt*$^{-/-}$ females in C, D, F, and G. The embryo in C is an example of what was scored as a severe zygotic *ppt*-like phenotype with a severely shortened trunk. The phenotypes of embryos in D and F resemble two of the extreme classes of dorsalized mutants, whereas the embryo in G has a partial secondary axis (center, foreground) branching off of the primary axis (left, background). The ectopic axis has a beating heart and otic vesicles, an arrowhead highlighting one otic vesicle. Whole mount in situ analysis of embryos from *ppt*$^{-/-}$ females. After photographing, genotypes were determined by PCR. mz-*ppt* represents maternal and zygotic loss of Wnt-5. Lateral view of 36 hpf embryos probed for the heart with Nkx2.5 in (H) wild-type and (I) mz-*ppt*, the black arrows show the endogenous heart, whereas the ectopic staining is noted with a white arrow. Animal pole view of embryos at 50% epiboly with dorsal to the right and arrowheads marking the lateral extent of the *chordin* expression domain in (J) wild-type, (K) mz-*ppt*, and in (L) mz-*ppt*, the star demarcates an ectopic domain.

(Schneider et al., 1996). To determine if there is a change at the level of β-catenin, embryos are analyzed for β-catenin protein distribution. In wild-type embryos, we typically observe nuclear β-catenin spanning ~20% the circumference of the embryo when observed from the animal pole. Fig. 5 A represents one frame of a confocal series at lower magnification with the regions of nuclear β-catenin localization (dots) confirmed at higher magnification. A representative frame from images collected around the circumference of a wild-type embryo at higher magnification is shown in Fig. 5 C with an arrowhead marking a cell with nuclear β-catenin. In wild type, we observe an average of 11 β-catenin-positive nuclei/embryo, (n = 10 embryos). In contrast, β-catenin-positive nuclei in embryos from $ppt^{-/-}$ females span >50% the embryo circumference, in some embryos, the domains are opposite the putative endogenous dorsal domain (Fig. 5 B, dots). Embryos from $ppt^{-/-}$ females demonstrate a dramatically higher number of cells with nuclear β-catenin (Average of 48 nuclei/embryo, n = 10 embryos) with a noticeable increase in the overall level of protein (Fig. 5 D, arrows denoting a few of the cells with nuclear β-catenin). The individual panels of wild type at higher magnification typically have 1–2 nuclei/frame in the dorsal domain, whereas *ppt* panels can have upwards of 6–10 nuclei/frame.

To analyze increased Wnt/β-catenin activity at the molecular level, we monitored expression of a downstream target, the homeodomain protein *bozozok* (Fekany et al., 1999). *boz* zygotic expression initiates at the dorsal blastoderm and dorsal YSL indicating the zebrafish organizer at 4 hpf (Fig. 6 A). 59% of embryos from $ppt^{-/-}$ females have expanded and/or ectopic *boz* expression (n = 147; Fig. 6, B–D). The $ppt^{-/-}$ embryos in Fig. 6 (B and C) display lateral expansion (arrowheads) of the *boz* expression domain as well as an increased number of *boz*-positive cells. Additionally ectopic domain of *boz* expression can be observed as a group of cells (Fig. 6 B) or as individual *boz*-positive cells (Fig. 6 D). Because a milder *ppt* allele (ppt^{ta89}) has redundant functions with *slb* in anterior cell movements (Kilian et al., 2003), we wanted to confirm genetic interaction between ppt^{ti265} and slb^{tz216} or potential functional redundancy between the Wnt-5 and -11 products in earlier embryonic stages. We evaluated *boz* distribution in embryos collected from a cross between doubly heterozygous ppt^{ti265} and slb^{tz216} parents. In the doubly homozygous ppt^{ti265}; slb^{tz216} mutant embryos, we observed an increase in the *boz* expression domain with a larger number of strongly expressing *boz*-positive cells forming a dark trapezoid shape (14%, n = 96; Fig. 6 F) compared with the linear pattern of weakly expressing *boz*-positive cells in wild-type (Fig. 6 E) and single mutant ppt^{ti265} or slb^{tz216} embryos (0%, n = 146). The mild increase in the *boz* expression domain suggests that there may be a zygotic contribution from this class of Wnts to maintain or refine, in part, the maternally established D-V boundaries.

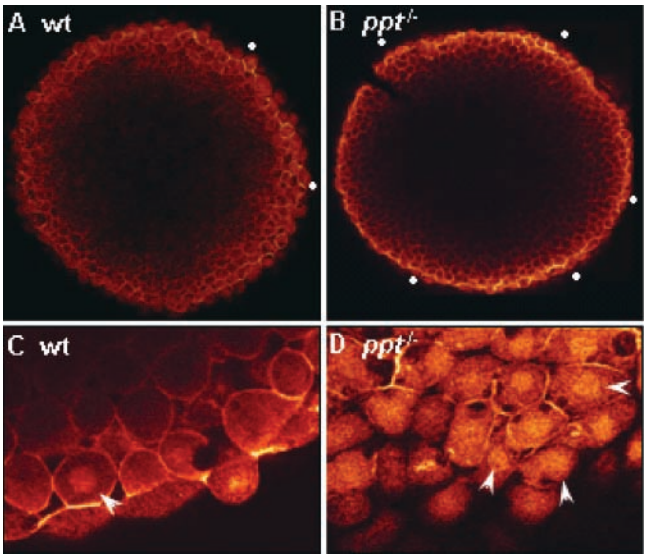

Figure 5. **Increased β-catenin protein and *boz* expression in Wnt-5/*ppt* mutant embryos.** Immunolocalization of β-catenin protein in sphere stage embryos. A panel from a confocal series collected with a 20× objective from (A) wild-type and (B) maternally depleted *ppt* embryos. White dots identify domains of nuclear β-catenin around the circumference of the embryos in an animal pole orientation. Additional confocal images were collected from the same embryos with a 63× objective. Representative β-catenin–positive nuclei noted by arrowheads with one B-catenin–positive nucleus in (C) wild-type and at least seven in (D) maternally depleted ppt embryo.

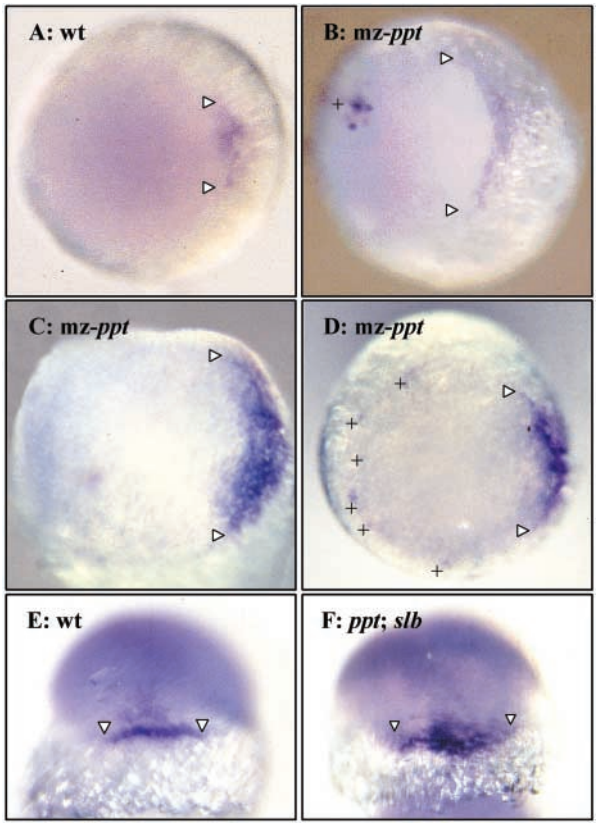

Figure 6. **Increased *boz* expression in Wnt-5/*ppt* mutant embryos.** Whole mount in situ hybridization with *boz*; animal pole view of (A) wild-type and (B-D) mz-*ppt* embryos; dorsal view of (E) wild-type and (F) ($ppt^{-/-}$;$slb^{-/-}$) embryos. The arrows mark the lateral extent of the *boz* expression domain and plus marks highlight ectopic domains.

CaMKII activity can partially rescue Wnt-5 (*ppt*) mutants

If the $ppt^{-/-}$ phenotype is the result of reduced Ca^{2+} release, it may be possible to suppress the mutant defect by artificially activating a Ca^{2+} cascade. CaM is a predominant Ca^{2+} binding protein in the cell, which, when bound to Ca^{2+}, stimulates CaM-dependent enzymes including Ca^{2+}/calmodulin-dependent protein kinases. Due to its proposed role in *Xenopus* ventral patterning (Kuhl et al., 2000a), we tested whether CaMKII was sufficient to rescue the Wnt-5 loss-of-function phenotype. Injection of full-length CaMKII, which should be under the control of endogenous Ca^{2+} modulation, did not alter the $ppt^{-/-}$ phenotype. Expression of an activated form of CaMKII, truncated to remove a regulatory domain (CamKIItr; Hansen et al., 2003), suppressed the $ppt^{-/-}$ phenotype (Fig. 7 B) compared with uninjected sibling $ppt^{-/-}$ embryos (Fig. 7 C). However, CaMKIItr expression did not completely rescue the phenotype relative to wild-type (Fig. 7 A). As in the Wnt-5 experiments, embryos from a standard *ppt* heterozygous cross were injected with CamKIItr and rescue was scored in injection sets with suppressed *ppt*-like tail and trunk phenotypes (*ppt* phenotypes in clutch controls are typically at 25%, whereas rescue sets had fewer than 10%). Embryos from injection sets with increased frequency of wild-type–like morphology were individually photographed and PCR genotyped. PCR genotype of wt-looking embryos revealed 19% homozygous *ppt* in CaMKIItr rescue sets, whereas no homozygous *ppt* genotypes were identified among phenotypic wild-type clutch embryos. Thus, constitutively active CaMKII can result in straightened tails and increased trunk length (within 90% of wt length). Additional rescued embryos ($n > 180$) were raised, whereas CaMKII-injected $ppt^{+/-}$ heterozygotes survived, no CaMKII-injected $ppt^{-/-}$ reached maturity.

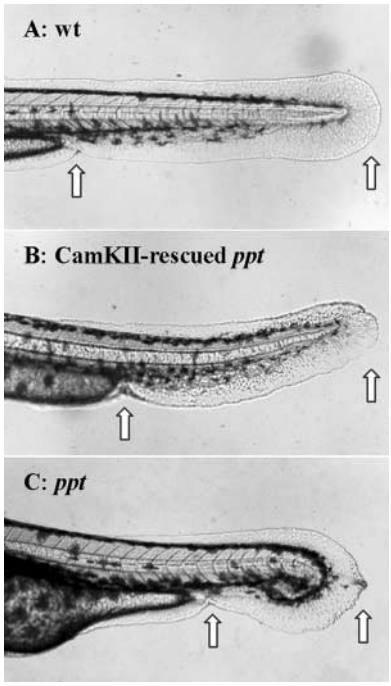

Figure 7. **Activated CaMKII suppresses the Wnt-5/$ppt^{-/-}$ tail defect.** Tail morphology of (A) wild-type, (B) CaMKIItr-rescued $ppt^{-/-}$, and (C) $ppt^{-/-}$ embryos are from the same clutch. Arrows denote the length from the end of the yolk tube to the tip of the tail. Zebrafish embryos from a standard *ppt* heterozygous cross were injected with CamKIItr. Injection sets with increased frequency of wild-type–like morphology (>90% compared with the expected 75%) were individually photographed and PCR genotyped.

Discussion

Recent work has highlighted the importance of Wnt/Ca^{2+} in ventral specification through misexpression of dominant negative Wnt-11, DN X nuclear factor of activated T cells and a truncated frizzled 8 in *Xenopus* (Itoh and Sokol, 1999; Kuhl et al., 2000a; Saneyoshi et al., 2002). A genetic loss of Wnt-5 function facilitates greater understanding of subcellular interactions, in the context of the whole embryo under endogenous regulatory dynamics. Our findings demonstrate that homozygous *ppt*/Wnt-5 mutant embryos have reduced frequency of Ca^{2+} release and mz*ppt*/Wnt-5 mutant embryos display hyperdorsalization phenotypes. The ectopic axes observed in mzppt^{ti265} embryos are partial, not complete axis duplications, possibly due to contributions from Wnt-11 or other maternally supplied Wnt/Ca^{2+} members. The synergy in the $ppt^{-/-}$;$slb^{-/-}$ double mutant suggests redundant/overlapping function with Wnt-11. Regardless, this is a genetic demonstration for a role of a Wnt in D-V patterning in vertebrate embryos.

Wnt-5 loss-of-function mimics activation of Wnt/β-catenin signaling most likely by relieving negative regulation of some component(s) of the Wnt–β-catenin pathway (Fig. 8). We observe an accumulation of β-catenin protein and ectopic activation of target genes. Although further studies in the mz-*ppt* embryos are needed to confirm if the impact on β-catenin and target genes is a direct effect of Wnt-5/Ca^{2+} activity, antagonism of β-catenin levels is consistent with Wnt-5 misexpression resulting in reduced chordin expres-

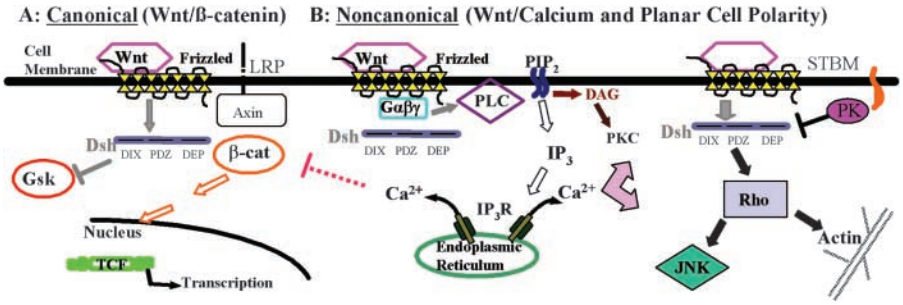

Figure 8. **Wnt signaling network.** Schematic of the stimulation of (A) canonical Wnt and (B) non-canonical Wnt/Ca^{2+} and planar cell polarity signaling pathways. (Note: only a few of the known components are outlined.)

sion domains. As there has not been a clear demonstration of a maternally provided canonical Wnt, the level of antagonism may lie within the cell. Recent demonstration of dsh activating Wnt/Ca^{2+} provides one candidate for maternal influence (Sheldahl et al., 2003). The cellular response to Ca^{2+} release most likely involves a network of proteins activating multiple components. Data suggests an antagonistic role for CaMKII, interfering with *Xenopus* gastrulation movements (Kuhl et al., 2001) and by CaMKII-dependent activation of a β-catenin/Tcf inhibiting nemolink kinase (Ishitani et al., 2003). The partial rescue of the $ppt^{-/-}$ phenotype suggests that although CaMKII is a downstream responder to Wnt/Ca^{2+} activation, other Ca^{2+}-sensitive components may also be required. In particular, PKC (Kuhl et al., 2001) and naked cuticle (Zeng et al., 2000; Yan et al., 2001) proteins, which could lead to β-catenin accumulation or those that could influence β-catenin nuclear import (Tolwinski et al., 2003), are perhaps required.

Misexpression of high levels of XWnt-5A with human Fz5 in frog embryos is sufficient to induce axis duplication (He et al., 1997). It is possible that, upon overexpression, Wnt5 and fz5 can stimulate both canonical and noncanonical Wnt pathways. However, misexpression of Wnt5 in melanoma cells activates PKC but not β-catenin and, furthermore, treatment of these melanoma cells with antibodies that block fz5 function show decreased Wnt-5A–induced PKC activation and metastasis (Weeraratna et al., 2002), supporting the hypothesis that the Fz5 couples into the Wnt–Ca^{2+} path. Whether axis duplication is the result of hyperactivation of the Wnt–Ca^{2+} path resulting in depletion of Ca^{2+} stores and subsequent Wnt/β-catenin activation or due to direct activation of the Wnt–β-catenin path has not been determined. Critical to the depletion hypothesis is that reduction of internal Ca^{2+} stores with the ER-specific Ca^{2+}-ATPase inhibitor thapsigargin results in hyperdorsalization (Westfall et al., 2003). In addition, we can activate Ca^{2+}-release frequency in vivo with low doses of Wnt-5 and hyperventralize embryos. Whether pathway specificity is at the level of ligand, the receptor, or elsewhere is an open question. Our genetic studies reveal an endogenous role for Wnt-5 in the early embryo but does not specifically address whether the phenotypes of individual Wnt genes depend on which fz (or low density lipoprotein receptor–related protein, for that matter) is expressed at particular developmental stages.

In summary, Wnt/Ca^{2+} functions in D-V axis specification. Our in vivo studies reveal that changes in intracellular Ca^{2+} concentrations as a result of Wnt-5 modulation can lead to rapid and sustained events by establishing feedback loops to sharpen boundaries or to coordinate cell movement. Wnt-5 is maternally required and its biological effects are in part due to negative regulation of Wnt/β-catenin signaling. Because activation of β-catenin signaling has been implicated in cancer, our work provides genetic evidence that the Wnt–Ca^{2+} pathway may be a tumor suppressor pathway. This is further supported by the recent demonstration that Ca^{2+} activity suppresses β-catenin in human colon carcinomas (Chakrabarty et al., 2003). Knowledge of the developmental processes of Wnt/Ca^{2+} signaling will lay the foundation for understanding complex developmental events, as well as the oncogenic role of the Wnt signaling family.

Materials and methods

Embryo manipulation

Fertilized eggs were collected from natural spawning of adults and microinjected with ~200 pl volumes at the 1-cell stage and 50–100 pl at the 8–32-cell stage. Capped RNA was prepared with the Ambion mMessage mMachine kit after template linearization. Wnt-4, -5, and -11 RNA was injected as ~200 pl drops of a 5–40-ng/μl stock solution. CaMKII and CaMKIItr (provided by S.H. Green, University of Iowa, Iowa City, IA) were injected at a 30–60-ng/μl stock solution. Wnt-5 DNA was injected at 8–12 ng/μl in a 100–200-pl drop. Live embryos were photographed with Nomarski optics after orienting in 3% methylcellulose and staged according to Kimmel et al. (1995).

Mutant identification

Stock families of heterozygous adults for ppt^{ti265} (Hammerschmidt et al., 1996), slb^{tz216} (Heisenberg et al., 1996), and ppt^{ti265};slb^{tz216} are maintained under standard conditions. Mutants are identified by test crosses back to ppt^{ti265};slb^{tz216}, as well as by PCR analysis. Genomic DNA isolated from single embryos or fin-snipped adults were proteinase K–treated (2 mg/ml in PCR buffer + Tween + NP-40). The PCR primers used for ppt^{ti265} in exon 4 (5′-CTACACCATCAGTATATTTCACC-3′ and 5′-CTATCAACGGCACACGTACAC-3′) identify an A to T transition at position 1045 and the primers specific for slb^{tz216} identify the truncation at glycine 155 (5′-AGCGTTTGTG GTTTCTCTGG-3′ and 5′-TCCTCATTGGTGCATCTGAG-3′). The PCR products were isolated and sequenced by standard techniques.

Pharmacological reagents

L-690,330 (Tocris), an inositol monophosphatase inhibitor (Atack et al., 1993), was injected to ~1.5–2 ng/embryo after the 8-cell stage. XeC (Calbiochem), a membrane-permeable blocker of IP_3-mediated Ca^{2+} release (Gafni et al., 1997), was used at 1–2 μM doses. For the cell movement defects, treatment was typically after the 128-cell stage.

Whole mount in situ hybridization

For all the manipulations, embryos at the appropriate developmental stage, sphere/dome or 50% epiboly, were placed in 4% PFA/PBS fixative. Digoxygenin-UTP RNA probes (Roche) were synthesized from linearized templates. Single probe hybridizations were done as described in Thisse et al. (1993) and double label in situ as described in Long and Rebagliati (2002). After probe detection, embryos were mounted and photographed.

β-Catenin immunolocalization

Embryos were fixed in 4% PFA/1× PBS at the sphere/dome stage. Overnight incubation with anti–β-catenin (P14L, provided by Dr. T. Kurth, MPI für Entwicklungsbiologie, Tübingen, Germany); Schneider et al., 1996), followed by secondary antibody conjugated with a fluorescent label (Texas-red or Alexa633; Molecular Probes). Nuclei were identified by counter stain with the 5 μM Sytox Green (Molecular Probes). Whole mount embryos in an animal pole orientation were optically sectioned using two-channel imaging on a scanning laser confocal microscope system (20×/0.7 Plan Apo and 63×/1.2 water objectives; model TCS-NT; Leica). The image stacks collected at 4-μm intervals were evaluated and nuclear β-catenin in nonoverlapping cells was counted as positive.

Calcium image analysis

The ratiometric Ca^{2+}-sensing dye Fura-2 (dextran conjugated; Molecular Probes) was injected into 1-cell zebrafish embryos. Indicated RNAs or pharmacological reagents were either coinjected with the Fura-2 at the 1-cell stage or unilaterally injected at the 8–16 cell stage mixed with dextran-conjugated Texas red lineage tracer (Molecular Probes) and imaged from 32 to 64 cell stage until beyond dome/early epiboly stages. Embryos collected from heterozygous *ppt* crosses were injected with Fura-2. The genotype of individual embryos was determined by PCR. Details of data collection and analysis are as described in Slusarski and Corces (2000). Ca^{2+} fluxes are determined by a subtractive analogue and represented as either a surface plot of Ca^{2+} activity across the embryo or a graphical representation of the number of new transients per image as a function of time.

We wish to thank B. Hjertos for earlier contributions to this work and Dr. M.E. Dailey for assistance with the confocal analysis. We also thank Dr. Y. Yang for sharing information before publication; and Dr. M. Rebagliati and Dr. R. Cornell for critical reading of the manuscript.

This work was supported by March of Dimes (MOD) (grant 5-FY99-806) and the American Cancer Society (grant IN-122V) administered through

the Holden Comprehensive Cancer Center at the University of Iowa. D.C. Slusarski is a MOD Basil O'Conner Research Scholar.

Submitted: 17 March 2003
Accepted: 2 July 2003

References

Ahumada, A., D.C. Slusarski, X.X. Liu, R.T. Moon, C.C. Malbon, and H.Y. Wang. 2002. Signaling of rat Frizzled-2 through phosphodiesterase and cyclic GMP. *Science.* 298:2006–2010.

Atack, J.R., S.M. Cook, A.P. Watt, S.R. Fletcher, and C.I. Ragan. 1993. In vitro and in vivo inhibition of inositol monophosphatase by the bisphosphonate L-690,330. *J. Neurochem.* 60:652–658.

Berridge, M.J., M.D. Bootman, and P. Lipp. 1998. Calcium-a life and death signal. *Nature.* 395:645–648.

Bienz, M., and H. Clevers. 2003. Armadillo/beta-catenin signals in the nucleus—proof beyond a reasonable doubt? *Nat. Cell Biol.* 5:179–182.

Blader, P., U. Strahle, and P.W. Ingham. 1996. Three *Wnt* genes expressed in a wide variety of tissues during development of the zebrafish, *Danio rerio*: developmental and evolutionary perspectives. *Development Genes and Evolution.* 206:3–13.

Buratovich, M.A., S. Anderson, K. Gieseler, J. Pradel, and E.L. Wilder. 2000. DWnt-4 and Wingless have distinct activities in the *Drosophila* dorsal epidermis. *Dev. Genes Evol.* 210:111–119.

Chakrabarty, S., V. Radjendirane, H. Appelman, and J. Varani. 2003. Extracellular calcium and calcium sensing receptor function in human colon carcinomas: promotion of E-cadherin expression and suppression of beta-catenin/TCF activation. *Cancer Res.* 63:67–71.

Chen, J.N., and M.C. Fishman. 1996. Zebrafish tinman homolog demarcates the heart field and initiates myocardial differentiation. *Development.* 122:3809–3816.

Cohen, E.D., M.C. Mariol, R.M.H. Wallace, J. Weyers, Y.G. Kamberov, J. Pradel, and E.L. Wilder. 2002. DWnt4 regulates cell movement and focal adhesion kinase during *Drosophila* ovarian morphogenesis. *Dev. Cell.* 2:437–448.

Dale, T. 1998. Signal transduction by the Wnt family of ligands. *Biochem. J.* 329: 209–223.

Du, S., S. Purcell, J. Christian, L. McGrew, and R. Moon. 1995. Identification of distinct classes and functional domains of Wnts through expression of wild-type and chimeric proteins in *Xenopus* embryos. *Mol. Cell. Biol.* 15:2625–2634.

Fekany, K., Y. Yamanaka, T. Leung, H.I. Sirotkin, J. Topczewski, M.A. Gates, M. Hibi, A. Renucci, D. Stemple, A. Radbill, et al. 1999. The zebrafish bozozok locus encodes Dharma, a homeodomain protein essential for induction of gastrula organizer and dorsoanterior embryonic structures. *Development.* 126:1427–1438.

Gafni, J., J.A. Munsch, T.H. Lam, M.C. Catlin, L.G. Costa, T.F. Molinski, and I.N. Pessah. 1997. Xestospongins: potent membrane permeable blockers of the inositol 1,4,5-trisphosphate receptor. *Neuron.* 19:723–733.

Gieseler, K., Y. Graba, M.C. Mariol, E.L. Wilder, A. Martinez-Arias, P. Lemaire, and J. Pradel. 1999. Antagonist activity of DWnt-4 and wingless in the *Drosophila* embryonic ventral ectoderm and in heterologous *Xenopus* assays. *Mech. Dev.* 85:123–131.

Hammerschmidt, M., F. Pelegri, M.C. Mullins, D.A. Kane, M. Brand, F.J. van Eeden, M. Furutani-Seiki, M. Granato, P. Haffter, C.P. Heisenberg, et al. 1996. Mutations affecting morphogenesis during gastrulation and tail formation in the zebrafish, Danio rerio. *Development.* 123:143–151.

Hansen, M.R., J. Bok, A.K. Devaiah, X.M. Zha, and S.H. Green. 2003. Ca^{2+}/calmodulin-dependent protein kinases II and IV both promote survival but differ in their effects on neurite growth in spiral ganglion neurons. *J. Neurosci. Res.* 72:169–184.

He, X., J.P. Saint-Jeannet, Y. Wang, J. Nathans, I. Dawid, and H. Varmus. 1997. A member of the Frizzled protein family mediating axis induction by Wnt-5A. *Science.* 275:1652–1654.

Heisenberg, C.P., and C. Nusslein-Volhard. 1997. The function of silberblick in the positioning of the eye anlage in the zebrafish embryo. *Dev. Biol.* 184:85–94.

Heisenberg, C.P., M. Brand, Y.J. Jiang, R.M. Warga, D. Beuchle, F.J. van Eeden, M. Furutani-Seiki, M. Granato, P. Haffter, M. Hammerschmidt, et al. 1996. Genes involved in forebrain development in the zebrafish, Danio rerio. *Development.* 123:191–203.

Heisenberg, C.P., M. Tada, G.J. Rauch, L. Saude, M.L. Concha, R. Geisler, D.L. Stemple, J.C. Smith, and S.W. Wilson. 2000. Silberblick/Wnt11 mediates convergent extension movements during zebrafish gastrulation. *Nature.* 405: 76–81.

Huelsken, J., and W. Birchmeier. 2001. New aspects of Wnt signaling pathways in higher vertebrates. *Curr. Opin. Genet. Dev.* 11:547–553 (Review).

Ishitani, T., S. Kishida, J. Hyodo-Miura, N. Ueno, J. Yasuda, M. Waterman, H. Shibuya, R.T. Moon, J. Ninomiya-Tsuji, and K. Matsumoto. 2003. The TAK1-NLK mitogen-activated protein kinase cascade functions in the Wnt-5A/Ca^{2+} pathway to antagonize Wnt/β-catenin signaling. *Mol. Cell. Biol.* 23:131–139.

Itoh, K., and S.Y. Sokol. 1999. Axis determination by inhibition of Wnt signaling in *Xenopus*. *Genes Dev.* 13:2328–2336.

Joly, J.S., C. Joly, S. Schulte-Merker, H. Boulekbache, and H. Condamine. 1993. The ventral and posterior expression of the zebrafish homeobox gene eve1 is perturbed in dorsalized and mutant embryos. *Development.* 119:1261–1275.

Kelly, G.M., P. Greenstein, D.F. Erezyilmaz, and R.T. Moon. 1995. Zebrafish *wnt-8* and *wnt-8b* share a common activity but are involved in distinct developmental pathways. *Development.* 121:1787–1799.

Kilian, B., H. Mansukoski, F.C. Barbosa, F. Ulrich, M. Tada, and C.P. Heisenberg. 2003. The role of Ppt/Wnt5 in regulating cell shape and movement during zebrafish gastrulation. *Mech. Dev.* 120:467–476.

Kimmel, C.B., W.W. Ballard, S.R. Kimmel, B. Ullmann, and T.F. Schilling. 1995. Stages of embryonic development of the zebrafish. *Dev. Dyn.* 203:253–310.

Kuhl, M., L.C. Sheldahl, C.C. Malbon, and R.T. Moon. 2000a. Ca^{2+}/calmodulin-dependent protein kinase II is stimulated by Wnt and Frizzled homologs and promotes ventral cell fates in *Xenopus*. *J. Biol. Chem.* 275:12701–12711.

Kuhl, M., L.C. Sheldahl, M. Park, J.R. Miller, and R.T. Moon. 2000b. The Wnt/Ca^{2+} pathway: a new vertebrate Wnt signaling pathway takes shape. *Trends Genet.* 16:279–283.

Kuhl, M., K. Geis, L.C. Sheldahl, T. Pukrop, R.T. Moon, and D. Wedlich. 2001. Antagonistic regulation of convergent extension movements in *Xenopus* by Wnt/beta-catenin and Wnt/Ca^{2+} signaling. *Mech. Dev.* 106:61–76.

Kume, S., A. Muto, T. Inooue, K. Suga, H. Okana, and K. Mikoshiba. 1997. Role of inositol 1,4,5-trisphosphate receptor in ventral signaling in *Xenopus* embryos. *Science.* 278:1940–1943.

Lele, Z., J. Bakkers, and M. Hammerschmidt. 2001. Morpholino phenocopies of the swirl, snailhouse, somitabun, minifin, silberblick, and pipetail mutations. *Genesis.* 30:190–194.

Long, S., and M. Rebagliati. 2002. Sensitive two-color whole-mount in situ hybridizations using digoxygenin- and dinitrophenol-labeled RNA probes. *Biotechniques.* 32:494, 496, 498.

Miller-Bertoglio, V.E., S. Fisher, A. Sanchez, M.C. Mullins, and M.E. Halpern. 1997. Differential regulation of chordin expression domains in mutant zebrafish. *Dev. Biol.* 192:537–550.

Mlodzik, M. 2002. Planar cell polarization: do the same mechanisms regulate *Drosophila* tissue polarity and vertebrate gastrulation? *Trends Genet.* 18:564–571.

Moon, R.T., and D. Kimelman. 1998. From cortical rotation to organizer gene expression: toward a molecular explanation of axis specification in *Xenopus*. *Bioessays.* 20:536–545.

Moon, R.T., R.M. Campbell, J.L. Christian, L.L. McGrew, J. Shih, and S. Fraser. 1993a. Xwnt-5A: a maternal Wnt that affects morphogenetic movements after overexpression in embryos of *Xenopus laevis*. *Development.* 119:97–111.

Moon, R.T., J.L. Christian, R.M. Campbell, L.L. McGrew, A.A. DeMarais, M. Torres, C.J. Lai, D.J. Olson, and G.M. Kelly. 1993b. Dissecting Wnt signaling pathways and Wnt-sensitive developmental processes through transient misexpression analyses in embryos of *Xenopus laevis*. *Dev. Suppl.* 85–94.

Mullins, M.C., M. Hammerschmidt, D.A. Kane, J. Odenthal, M. Brand, F.J. van Eeden, M. Furutani-Seiki, M. Granato, P. Haffter, C.P. Heisenberg, et al. 1996. Genes establishing dorsoventral pattern formation in the zebrafish embryo: the ventral specifying genes. *Development.* 123:81–93.

Olson, D.J., and D.M. Gibo. 1998. Antisense wnt-5a mimics wnt-1-mediated C57MG mammary epithelial cell transformation. *Exp. Cell Res.* 241:134–141.

Rauch, G.J., M. Hammerschmidt, P. Blader, H.E. Schauerte, U. Strahle, P.W. Ingham, A.P. McMahon, and P. Haffter. 1997. Wnt5 is required for tail formation in the zebrafish embryo. *Cold Spring Harb. Symp. Quant. Biol.* 62: 227–234.

Sakaguchi, T., T. Mizuno, and H. Takeda. 2002. Formation and patterning roles of the yolk syncytial layer. *Results Probl. Cell Differ.* 40:1–14.

Saneyoshi, T., S. Kume, Y. Amasaki, and K. Mikoshiba. 2002. The Wnt/calcium pathway activates NF-AT and promotes ventral cell fate in *Xenopus* embryos.

Nature. 417:295–299.

Schneider, S., H. Steinbeisser, R.M. Warga, and P. Hausen. 1996. Beta-catenin translocation into nuclei demarcates the dorsalizing centers in frog and fish embryos. *Mech. Dev.* 57:191–198.

Sheldahl, L.C., M. Park, C.C. Malbon, and R.T. Moon. 1999. Protein kinase C is differentially stimulated by Wnt and Frizzled homologs in a G-protein-dependent manner. *Curr. Biol.* 9:695–698.

Sheldahl, L.C., D.C. Slusarski, P. Randur, J.R. Miller, M. Kuhl, and R.T. Moon. 2003. Dishevelled activates Ca^{2+} flux, PKC, and CamKII in vertebrate embryos. *J. Cell Biol.* 161:769–777.

Slusarski, D.C., and V.G. Corces. 2000. Calcium imaging in cell-cell signaling. *In* Developmental Biology Protocols. Vol. 1. R.S. Tuan and C.W. Lo, editors. Humana Press, Totowa, NJ. 253–261.

Slusarski, D.C., V.G. Corces, and R.T. Moon. 1997a. Interaction of Wnt and a Frizzled homologue triggers G-protein-linked phosphatidylinositol signalling. *Nature.* 390:410–413.

Slusarski, D.C., J. Yang-Snyder, W.B. Busa, and R.T. Moon. 1997b. Modulation of embryonic intracellular Ca^{2+} signaling by Wnt-5A. *Dev. Biol.* 182:114–120.

Thisse, C., B. Thisse, T.F. Schilling, and J.H. Postlethwait. 1993. Structure of the zebrafish snail1 gene and its expression in wild-type, spadetail and no tail mutant embryos. *Development.* 119:1203–1215.

Tolwinski, N.S., M. Wehrli, A. Rives, N. Erdeniz, S. DiNardo, and E. Wieschaus. 2003. Wg/Wnt signal can be transmitted through arrow/LRP5,6 and Axin independently of Zw3/Gsk3beta activity. *Dev. Cell.* 4:407–418.

Ungar, A.R., and R.T. Moon. 1995. Wnt4 affects morphogenesis when misexpressed in the zebrafish embryo. *Mech. Dev.* 52:153–164.

Veeman, M.T., D.C. Slusarski, A. Kaykas, S.H. Louie, and R.T. Moon. 2003. Zebrafish prickle, a modulator of noncanonical wnt/fz signaling, regulates gastrulation movements. *Curr. Biol.* 13:680–685.

Weeraratna, A.T., Y. Jiang, G. Hostetter, K. Rosenblatt, P. Duray, M. Bittner, and J.M. Trent. 2002. Wnt5a signaling directly affects cell motility and invasion of metastatic melanoma. *Cancer Cell.* 1:279–288.

Westfall, T.A., B. Hjertos, and D.C. Slusarski. 2003. Requirement for intracellular calcium modulation in zebrafish dorsal-ventral patterning. *Dev. Biol.* 259: 380–391.

Yan, D., J.B. Wallingford, T.Q. Sun, A.M. Nelson, C. Sakanaka, C. Reinhard, R.M. Harland, W.J. Fantl, and L.T. Williams. 2001. Cell autonomous regulation of multiple dishevelled-dependent pathways by mammalian Nkd. *Proc. Natl. Acad. Sci. USA.* 98:3802–3807.

Zeng, W.L., K.A. Wharton, J.A. Mack, K. Wang, M. Gadbaw, K. Suyama, P.S. Klein, and M.P. Scott. 2000. Naked cuticle encodes an inducible antagonist of Wnt signalling. *Nature.* 403:789–795.